# Free-Standing and Oriented Periodic Mesoporous Organosilica Films with Variable Pore Size at the Air−Water Interface

Sung Soo Park and Chang-Sik Ha*

*Department of Polymer Science and Engineering, Pusan National University, Pusan 609-735, Korea*

*Received March 10, 2005. Revised Manuscript Received May 4, 2005*

Free-standing and oriented periodic mesoporous organosilica (PMO) films with variable pore size have been synthesized at the air−water interface using cationic alkyltrimethylammonium surfactants (alkyl chain length from 12 to 18 carbon atoms) as the structure-directing agents and 1,2-bis(triethoxysilyl)-ethane as the organosilica precursor. After hydrothermal reaction at 95 °C for 8 h, $C_{12}$TA−PMO, $C_{16}$-TA−PMO, and $C_{18}$TA−PMO films grown at the air−water interface have a uniform thickness of ∼350, ∼670, and ∼400 nm, respectively. From the XRD patterns and TEM images, PMO films with hexagonal symmetry were identified. It was confirmed by $^{29}$Si and $^{13}$C CP MAS NMR experiments that the organic−inorganic moiety (−Si−$CH_2$−$CH_2$−Si−) is the basic structural unit in the films. The pore diameter and the surface area of the surfactant-extracted PMO films, e.g., $C_{12}$TA−, $C_{16}$TA−, and $C_{18}$TA−PMO films, obtained from the $N_2$ sorption isotherms were to be determined to be 24.3, 26.4, and 32.8 Å and 890.3, 917.7, and 811.0 $m^2$ $g^{-1}$, respectively.

## Introduction

In recent years, surfactant-templated binuclear alkoxysilane precursors, $(R'O)_3Si-R-Si(OR')_3$, lead to a new class of nanocomposites with bridging organic groups (R) inside the channel walls,[1−5] called periodic mesoporous organosilica (PMO). These PMO materials facilitate chemistry of the channels and provide new opportunities for controlling the chemical, physical, mechanical, and dielectric properties of the materials.[6−9] Recently, mesoporous organosilica films were synthesized through a surfactant-templated self-assembly procedure using the hydrolysis and condensation of an alkoxysilane with a bridging organic group ($(R'''O)_3Si-R''-Si(OR''')_3$) (R''' = $-CH_3$ or $-C_2H_5$, R'' = ethane, ethylene, thiophene, and benzene)[10] or a cyclic siliquioxane precursor ($[(EtO)_2SiCH_2]_3$).[11] These films have low dielectric constants and good mechanical stability. Yu et al.[12a] and de Theije et al.[12b] reported the synthesis of mesoporous low dielectric constant organosilica films containing $SiO_3R''''$-(R'''' = $-CH_3$, −N═C═O) in a silica and polymer matrix. These mesoporous organosilica films were placed onto solid substrates such as silicon wafers or glass slides using spin- or dip-coating methods. Three groups[13] have reported the formation of ordered mesoporous silica films at the air−water interface. Recently, we described a surfactant-templated synthesis of high-quality free-standing and oriented PMO films grown at the air−water interface.[14] To the best of our knowledge, however, no work has yet been reported on the synthesis of mesoporous organosilica film with controllable pore size without a solid substrate grown at the air−water interface. In this paper, we report the first successful control of the pore size of free-standing and oriented PMO films grown at the air−water interface using cationic alkyltrimethylammonium surfactants (alkyl chain length from 12 to 18 carbon atoms) as the structure-directing agents.

* Corresponding author. Fax: +82 51 513 4331. Tel: +82 51 510 2407. E-mail: csha@pusan.ac.kr.

(1) (a) Inagaki, S.; Guan, S.; Fukushima, Y.; Ohsuna, T.; Terasaki, O. *J. Am. Chem. Soc.* **1999**, *121*, 9611. (b) Melde, B. J.; Holland, B. T.; Blanford, C. F.; Stein, A. *Chem. Mater.* **1999**, *11*, 3302. (c) Asefa, T.; MacLachian, M. J.; Coombs, N.; Ozin, G. A. *Nature* **1999**, *402*, 867.

(2) (a) Stein, A.; Melde, B. J.; Schroden, R. C. *Adv. Mater.* **2000**, *12*, 1403. (b) Asefa, T.; Ozin, G. A.; Grondey, H.; Kruk, M.; Jaroniec, M. *Stud. Surf. Sci. Catal.* **2002**, *141*, 1.

(3) Inagaki, S.; Guan, S.; Ohsuna, T.; Terasaki, O. *Nature* **2002**, *416*, 304.

(4) Kapoor, M. P.; Inagaki, S. *Chem. Mater.* **2002**, *14*, 3509.

(5) (a) Guo, W.; Park, J. Y.; Oh, M. O.; Jeong, H. W.; Cho, W. J.; Kim, I.; Ha, C. S. *Chem. Mater.* **2003**, *15*, 2295. (b) Guo, W.; Kim, I.; Ha, C. S. *Chem. Commun.* **2003**, 2692.

(6) Fukuoka, A.; Sakamoto, Y.; Guan, S.; Inagaki, S.; Sugimoto, N.; Fukushima, Y.; Hirahara, K.; Iijima, S.; Ichikawa, M. *J. Am. Chem. Soc.* **2001**, *123*, 3373.

(7) Burleigh, M. C.; Dai, S.; Hagaman, E. W.; Lin, J. S. *Chem. Mater.* **2001**, *13*, 2537.

(8) Yang, Q.; Kapoor, M. P.; Inagaki, S. *J. Am. Chem. Soc.* **2002**, *124*, 9694.

(9) (a) Yamamoto, K.; Nohara, Y.; Tatsumi, T. *Chem. Lett.* **2001**, 648. (b) Kapoor, M. P.; Bhaumik, A.; Inagaki, S.; Kuraoka, K.; Yazawa, T. *J. Mater. Chem.* **2002**, *12*, 3078. (c) Bhaumik, A.; Kapoor, M. P.; Inagaki, S. *Chem. Commun.* **2003**, 470.

(10) (a) Lu, Y.; Fan, H.; Doke, N.; Loy, D. A.; Assink, R. A.; LaVan, D. A.; Brinker, C. J. *J. Am. Chem. Soc.* **2000**, *122*, 5258. (b) Dag, Ö.; Yoshina-Ishii, C.; Asefa, T.; MacLachlan, M. J.; Grondey, H.; Coombs, N.; Ozin, G. A. *Adv. Funct. Mater.* **2001**, *11*, 213.

(11) Landskron, K.; Hatton, B. D.; Perovic D. D.; Ozin, G. A. *Science* **2003**, *302*, 266.

(12) (a) Yu, S.; Wong, T. K. S.; Hu, X.; Pita, K. *Chem. Phys. Lett.* **2004**, *384*, 63. (b) de Theije, F. K.; Balkenende, A. R.; Verheijen, M. A.; Baklanov, M. R.; Mogilnikov, K. P.; Furukawa, Y. *J. Phys. Chem. B* **2003**, *107*, 4280.

(13) (a) Yang, H.; Coombs, N.; Sokolov, I.; Ozin, G. A. *Nature* **1996**, *381*, 589. (b) Ruggles, J. L.; Holt, S. A.; Reynolds, P. A.; Brown, A. S.; Creagh, D. C.; White, J. W. *Phys. Chem. Chem. Phys.* **1999**, *1*, 323. (c) Tolbert, S. H.; Schäffer, T. E.; Feng, J.; Hansma, P. K.; Stucky, G. D. *Chem. Mater.* **1997**, *9*, 1962.

(14) Park, S. S.; Ha, C.-S. *Chem. Commun.* **2004**, 1986.

10.1021/cm050548a CCC: $30.25 
Published on Web 05/28/2005

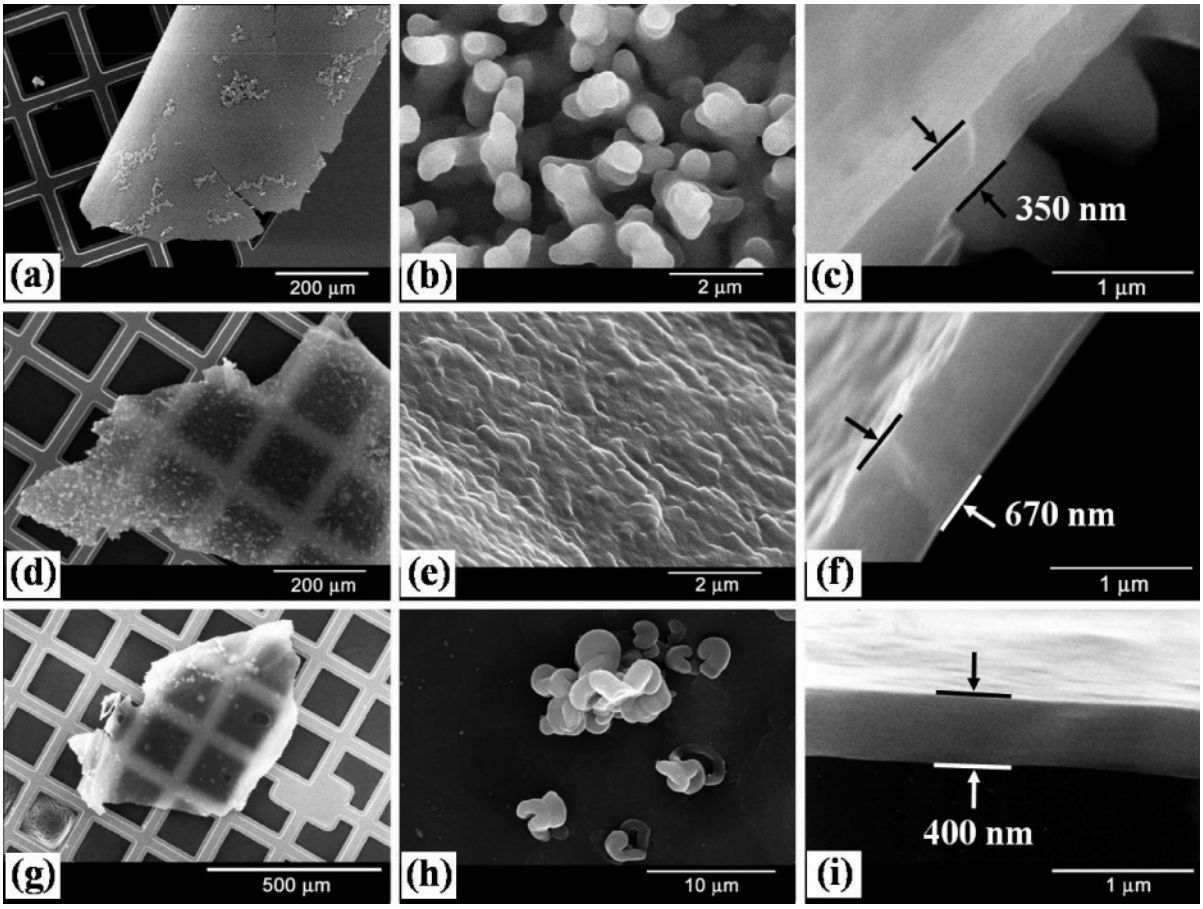


**Figure 1.** SEM images of as-synthesized free-standing (a) $C_{12}$TA−, (d) $C_{16}$TA−, and (g) $C_{18}$TA−PMO films transferred from the air−water interface onto a copper grid, magnified surface ((b), (e), and (h)), and edge part ((c), (f), and (i)) of sample (a), (d), and (g), respectively.

## Experimental Section

**Chemicals.** Dodecyltrimethylammonium bromide ($C_{12}$TABr, 99%, Aldrich), cetyltrimethylammonium bromide ($C_{16}$TABr, ≥99%, Fluka), and octadecyltrimethylammonium bromide ($C_{18}$TABr, Aldrich) as structure-directing agents and 1,2-bis(triethoxysilyl)ethane (BTSE, 96%, Aldrich) as organosilica source reagents were used. Sodium hydroxide (95%, Katayama chemical), and absolute ethanol (99.9% (v/v), Hayman) were purchased. All chemicals were used as purchased.

**Synthesis of PMO Films with Variable Pore Size at the Air−Water Interface.** The synthesis of PMO films with variable pore diameters at the air−water interface is achieved using the following reactant molar ratios and synthesis procedure: BTSE:surfactant:NaOH:$H_2O$; ($C_{12}$TABr): 1.0:0.57:2.36:353 ($C_{12}$TA−PMO), ($C_{16}$TABr): 1.0:0.57:2.28:336 ($C_{16}$TA−PMO), ($C_{18}$TABr): 1.0:0.57:2.36:353 ($C_{18}$TA−PMO), where $C_{12}$TABr, $C_{16}$TABr, and $C_{18}$TABr are the cationic surfactants $CH_3(CH_2)_{11}N(CH_3)_3Br$, $CH_3(CH_2)_{15}N(CH_3)_3Br$, and $CH_3(CH_2)_{17}N(CH_3)_3Br$, respectively, and BTSE is the organosilica source reagent $(C_2H_5O)_3SiCH_2CH_2Si(OC_2H_5)_3$. Typically, we synthesized the PMO films in a 50 mL polypropylene (PP) bottle (diameter, 4.5 cm) with 1/353 scale of the reactant mole ratios. The surfactant solution is mixed with BTSE and stirred at 40 °C for 12 h and heated at 95 °C for 8 h in the PP bottle. PMO films, with pore diameter from 24.3 to 32.8 Å, have been grown at the air−liquid interface. The PMO films were rinsed with distilled water and dried at 80 °C in air. The PMO films can be transferred from the air−water interface onto a substrate such as a silicon wafer or a slide glass etc. by the "pull-up" technique. The surfactant in the PMO films was removed by a solvent extraction process with 150 mL of EtOH including 3 mL of 35 wt % HCl at 60 °C for 12 h and dried at 80 °C for 12 h.

**Characterization.** The powder X-ray diffraction (XRD) patterns were obtained by using a Rigaku Miniflex diffractometer (40 kV, 30 mA) with Cu Kα radiation of wavelength 1.541 Å. The scan speed was 0.02/min in the $2\theta$ range from 1.5 to 10°. The adsorption and desorption isotherms of nitrogen at −196 °C were measured using a Micromeritics ASAP2010 instrument. All samples were outgassed at 150 °C for 12 h under vacuum ($p < 5 \times 10^{-6}$ Torr) in the degas port of the adsorption analyzer. The pore size distribution curve was obtained from an analysis of the desorption branch by using the Barrett−Joyner−Halenda (BJH) method. Scanning electron microscopy (SEM) images were obtained using a KEVEX Sigma microscope with an acceleration voltage of 20 kV. The samples were coated with gold using an Hitachi E-1010 sputter coater prior to imaging. Transmission electron microscopy (TEM) images were obtained using a JEOL JEM-2010 microscope operating at 200 kV. $^{29}$Si and $^{13}$C cross polarization (CP) MAS NMR spectra were obtained on a Bruker DSX400 spectrometer at room temperature with a 4 mm zirconia rotor spinning at 6 kHz (resonance frequencies of 79.5 and 100.6 MHz for $^{29}$Si and $^{13}$C CP MAS

**Table 1. Relative Yields of the Bulk Product PMO and the PMO Film**

| | yield | | |
|---|---|---|---|
| | | relative yields (mol %) | |
| sample name | total yield (mol %) | bulk product PMO[a] | PMO film |
| $C_{12}$TMA−PMO film | 55.9 | 96.7 | 3.3 |
| $C_{16}$TMA−PMO film | 78.2 | 97.8 | 2.2 |
| $C_{18}$TMA−PMO film | 70.0 | 97.3 | 2.7 |

[a] The bulk product PMO precipitated on the bottom of the PP bottle during the PMO film synthesis.

NMR, respectively; 90° pulse width of 5 $\mu$s, contact time 2 ms, recycle delay 3 s for both $^{29}$Si and $^{13}$C CP MAS NMR).

## Results and Discussion

Scanning electron microscopy (SEM) images of the PMO films that have been transferred onto a copper grid revealed that they are continuous, as shown in Figure 1. The size of the films that are formed at the air−water interface is dependent on the breadth of the reaction bottle. Figure 1a, d, and g show low-magnification SEM images of the PMO films synthesized at the air−water interface using cationic alkyltrimethylammonium surfactants with alkyl chain length of 12, 16, and 18 carbon atoms as structure-directing agents, respectively. When these three kinds of films were synthesized, precipitates were also formed on the bottom of the reaction bottle. The yields of the PMO films and the bulk product PMO precipitated on the bottom of the PP bottle are summarized in Table 1. During the hydrothermal reaction, the precipitates aggregated on the surface of the PMO films, as shown in Figure 1b, e, and h. The $C_{12}$TA−PMO, $C_{16}$TA−PMO, and $C_{18}$TA−PMO films have uniform thickness of ∼350, ∼670, and ∼400 nm, as shown in SEM images in Figure 1c, f, and i, respectively.

The as-synthesized free-standing PMO films were lifted onto transmission electron microscopy (TEM) grids and viewed directly. The TEM images of $C_{12}$TA−PMO, $C_{16}$TA−PMO, and $C_{18}$TA−PMO films showed that the films have a highly ordered periodic structure with a hexagonal closed-packed arrangement of channels running parallel to the surface of the films, as shown in Figure 2a, c, and e, respectively. This implies growth of the channels in an orientation parallel to the air−water interface. The periodicity with a hexagonal close-packed arrangement of one-dimensional channels viewed orthogonally to the film surface was observed at the bent edge part of the films, as shown in Figure 1b, d, and f, respectively.

Figure 3 shows TEM images of the calcined PMO films at 400 °C for 2 h in $N_2$. After calcination, the mesostructure of the $C_{12}$TA− (Figure 3a and b), $C_{16}$TA− (Figure 3c and d), and $C_{18}$TA−PMO (Figure 3e and f) films was retained with a well-ordered periodic structure consistent with a hexagonal close-packed arrangement.

Figure 4a, b, and c show the X-ray diffraction (XRD) patterns for the as-synthesized free-standing films, e.g., $C_{12}$TA−, $C_{16}$TA−, and $C_{18}$TA−PMO films, respectively, lifted onto a slide glass substrate. The $C_{16}$TA− and $C_{18}$TA−PMO films both reveal (100) and (200) reflections, consistent with the TEM observation that the channels run parallel to the surfactant overlayer at the air−water interface, as shown in Figure 2c and e, respectively. In the case of the $C_{12}$TA−PMO film, only the (100) peak was observed. As expected, the *d* spacing increases with longer alkyl chains in the structure-directing agent. The as-synthesized $C_{12}$TA−, $C_{16}$TA−, and $C_{18}$TA−PMO films have *d* spacings of 40.1, 43.7, and 47.7 Å, as obtained from the (100) reflection, respectively. The starred peaks are due to extra surfactants. These peaks nearly disappeared after calcination at 400 °C for 2 h in $N_2$ without cracking or loss of mesostructure, which is consistent with the XRD results in Figure 4d, e, and f and the TEM images in Figure 3b, d, and f, the $C_{16}$TA− (Figure 4e), and $C_{18}$TA−PMO (Figure 4f) films all reveal (100) and (200) reflections. On calcination of the films, the intensities of the peaks are increased and the anticipated contractions of the hexagonal *ab*-unit cell are observed, due to the removal of the surfactant template from the channels, which is concomitant with the condensation of the silanol (SiOH) groups in the channel walls.[10b,13a] The calcined $C_{12}$TA−, $C_{16}$TA−, and $C_{18}$TA−PMO films have *d* spacings of 39.1, 41.3, and 46.5 Å, as obtained from the (100) reflection, respectively. The inset in Figure 4 shows the XRD patterns of powdered and surfactant-extracted $C_{12}$TA− (Figure 4g), $C_{16}$TA− (Figure 4h), and $C_{18}$TA−PMO (Figure 4i) films, respectively. The XRD patterns of powdered and surfactant-extracted $C_{16}$TA− and $C_{18}$TA−PMO films showed the expected (100, 110, 200) reflections typically observed in powder PMO materials.[15] In the case of the powdered and surfactant-extracted $C_{12}$TA−PMO film, the (110) and (200) peaks of around $2\theta = 4°$ were not well-resolved due to the

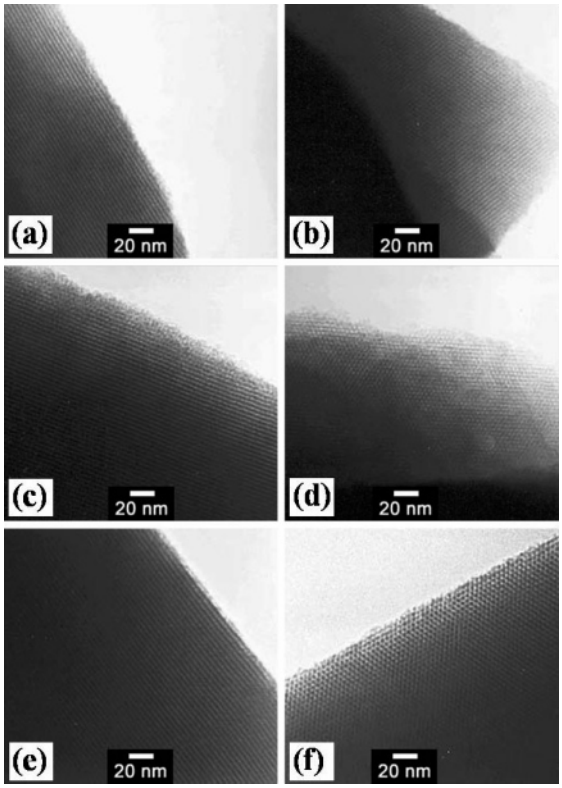


**Figure 2.** TEM images of as-synthesized ((a), (b)) $C_{12}$TA−, ((c), (d)) $C_{16}$TA−, and ((e), (f)) $C_{18}$TA−PMO films, showing ((a), (c), and (e)) a highly ordered periodic structure consistent with a hexagonal close-packed arrangement of channels running parallel to the surface of the film and ((b), (d), and (f)) hexagonal basal plane with a well-ordered hexagonal array.

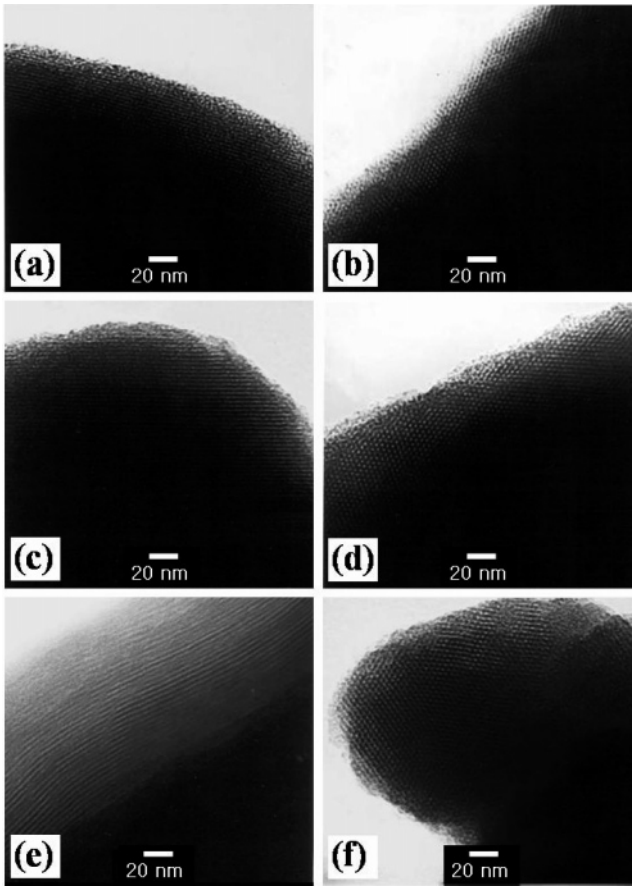


**Figure 3.** TEM images of calcined ((a), (b)) $C_{12}TA-$, ((c), (d)) $C_{16}TA-$, and ((e), (f)) $C_{18}TA-PMO$ films at 400 °C for 2 h in $N_2$, showing ((a), (c), and (e)) a highly ordered periodic structure consistent with a hexagonal close-packed arrangement of channels running parallel to the surface of the film and ((b), (d), and (f)) hexagonal basal plane with a well-ordered hexagonal array.

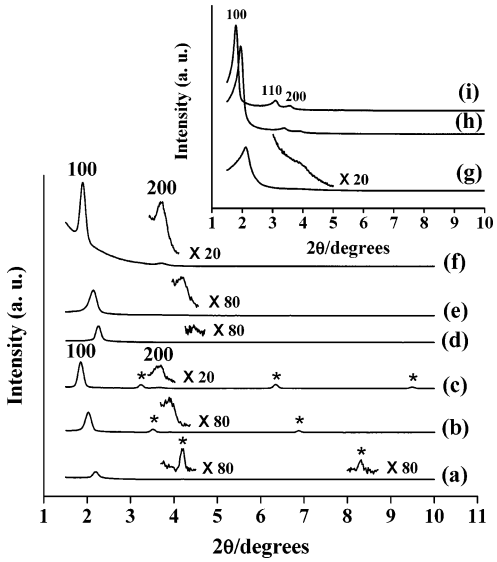


**Figure 4.** XRD patterns of as-synthesized free-standing (a) $C_{12}TA-$, (b) $C_{16}TA-$, and (c) $C_{18}TA-PMO$ films transferred from the air−water interface onto glass substrate, and calcined PMO films ((d), (e), and (f)) at 400 °C for 2 h in $N_2$ with sample (a), (b), and (c), respectively. Inset shows XRD patterns of powdered and surfactant-extracted (g) $C_{12}TA-$, (h) $C_{16}TA-$, and (i) $C_{18}TA-PMO$ films.

short-range structural order compared to the $C_{16}TA-$ and $C_{18}TA-PMO$ films. The pore diameter and the surface area of the surfactant-extracted PMO films, e.g., $C_{12}TA-$, $C_{16}TA-$, and $C_{18}TA-PMO$ films, obtained from the $N_2$ sorption isotherms were determined to be 24.3, 26.4, and 32.8 Å and 890.3, 917.7, and 811.0 $m^2\ g^{-1}$, respectively (Figure 5).

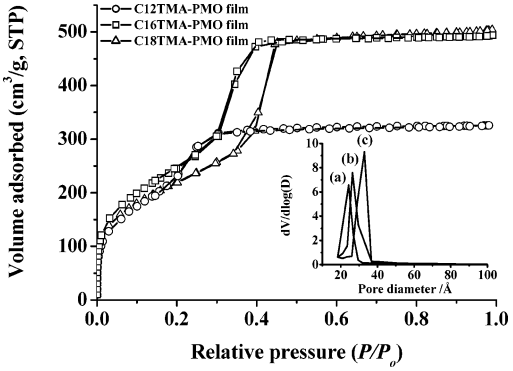


**Figure 5.** Nitrogen adsorption−desorption isotherms for surfactant-extracted PMO films. Inset shows the pore size distribution obtained using desorption branch by BJH method: (a) $C_{12}TA-$, (b) $C_{16}TA-$, and (c) $C_{18}TA-PMO$ films.

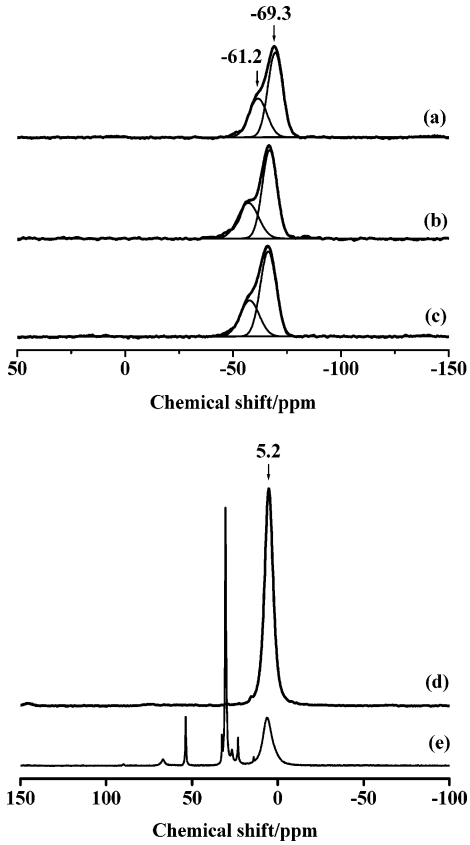


**Figure 6.** $^{29}Si$ MAS NMR spectra of (a) as-synthesized, (b) surfactant-extracted, and (c) calcined at 400 °C for 2 h in $N_2$ $C_{18}TA-PMO$ film and $^{13}C$ cross-polarization (CP) MAS NMR spectra of (d) surfactant-extracted and (e) as-synthesized $C_{18}TA-PMO$ film.

The Si−C bonding in the framework of the PMO film was confirmed by $^{29}Si$ and $^{13}C$ CP MAS NMR experiments, as shown in Figure 6. The $^{29}Si$ MAS NMR spectrum of the as-synthesized PMO film (Figure 6a) shows two peaks at −61.2 and −69.3 ppm, which can be assigned to $T^2$ $C(OH)Si(OSi)_2$ and $T^3$ $CSi(OSi)_3$.[1a,b] The $^{13}C$ CP MAS NMR spectroscopy of the as-synthesized PMO film exhibits a peak at 6.3 ppm, which is attributed to carbon covalently linked

(15) Park, S. S.; Lee, C. H.; Cheon, J. H.; Park, D. H. *J. Mater. Chem.* **2001**, *11*, 3397.

to Si (Si−$CH_2$−$CH_2$−Si) (Figure 6e).[1a,b] Peaks due to surfactant carbon atoms were observed at 14.1, 23.2, 26.7, 30.5, 32.6, 53.7, and 67.0 ppm.[3,4] After surfactant extraction, the $^{29}$Si MAS NMR spectrum shows two signals at −57.5 and −66.9 ppm which are assigned to $T^2$ $C(OH)Si(OSi)_2$ and $T^3$ $CSi(OSi)_3$, as shown in Figure 6b. The $^{13}$C CP MAS NMR spectrum shows a strong single resonance at 5.2 ppm, which is attributed to carbon covalently linked to Si (Si−$CH_2$−$CH_2$−Si), as shown in Figure 6d. It was confirmed by NMR experiments that the organic−inorganic moiety (−Si−$CH_2$−$CH_2$−Si−) is the basic structural unit in the film. The PMO film was calcined at 400 °C in $N_2$ and investigated by $^{29}$Si MAS NMR spectroscopy (Figure 6c). The spectrum shows two peaks ($T^2$ and $T^3$), indicating that the Si−C bonds remained intact. The fraction of $T^3$ obtained from the fitted curves for the calcined PMO film (33.8% and 66.2% for $T^2$ and $T^3$, respectively) is higher than that of the as-synthesized PMO film (35.9% and 64.1 for $T^2$ and $T^3$, respectively), which is consistent with the XRD results for the film (i.e., the decreasing *d* spacing after calcination). The fraction of $T^3$ obtained from the fitted curves for the surfactant-extracted PMO film (35.8% and 64.2% for $T^2$ and $T^3$, respectively) is similar to that of the as-synthesized PMO film.

Yang et al.[13a] reported that the formation of a mesoporous silica film involves collective interactions between silicate building blocks, micellar solution species, and a surfactant "hemi-micellar" overstructure localized at the air−water interface. The PMO film growth is probably regulated by matching charge and geometry between micellar aggregates and organosilica precursors at a surfactant-structured air−water interface, as suggested in the case of silica films.

## Conclusions

In conclusion, for the first time, free-standing and oriented PMO films with variable pore diameters were successfully synthesized at the air−water interface using cationic alkyltrimethylammonium surfactants (alkyl chain length from 12 to 18 carbon atoms) as the structure-directing agents and 1,2-bis(triethoxysilyl)ethane as the organosilica precursor. The films have a hexagonal mesostructure, with the organic moiety inside the channel wall. The films are continuous over the entire bulk, depending on the size of the reaction bottle. The PMO films may have potential use in applications such as catalysis, sensing, and separation.

**Acknowledgment.** This work was supported by the National Research Laboratory Program, the Center for Integrated Molecular Systems, and the BK21 Project.

CM050548A